Mg–C System up to 20 GPa: Its Phase Diagram and Stable Magnesium Carbides

Vladimir Z Turkevich, Carlos Renero-Lecuna, Yixuan Zhao, Yann Le Godec, Timothy A Strobel, Wilson A Crichton, Nicolas Guignot, Hicham Moutaabbid, Ioannis Touloupas, Alexandre Courac

THE JOURNAL OF PHYSICAL CHEMISTRY C
A JOURNAL OF THE AMERICAN CHEMICAL SOCIETY

pubs.acs.org/JPCC

Article

Mg−C System up to 20 GPa: Its Phase Diagram and Stable Magnesium Carbides

Vladimir Z. Turkevich, Carlos Renero-Lecuna, Yixuan Zhao, Yann Le Godec, Timothy A. Strobel, Wilson A. Crichton, Nicolas Guignot, Hicham Moutaabbid, Ioannis Touloupas, and Alexandre Courac*

Cite This: https://doi.org/10.1021/acs.jpcc.2c07176

Read Online

ACCESS | Metrics & More | Article Recommendations | Supporting Information

ABSTRACT: The phase diagram of the Mg−C system has been constructed up to 20 GPa and ∼4000 K based on complementary Thermo-Calc simulations and experimental data obtained in both *ex situ* and *in situ* experiments using X-ray diffraction with synchrotron radiation. Three high-pressure magnesium carbides, namely, β-Mg_2C_3, its high-temperature form γ-Mg_2C_3, and antifluorite Mg_2C, have $p-T$ domains of thermodynamic stability. At the same time, the carbides accessible by ambient-pressure synthesis, α-Mg_2C_3 and MgC_2, are either metastable or unstable, depending on the temperature, at least up to 20 GPa. Experimental observations show that at ambient conditions, all carbides are metastable and remain unchanged at least for years.

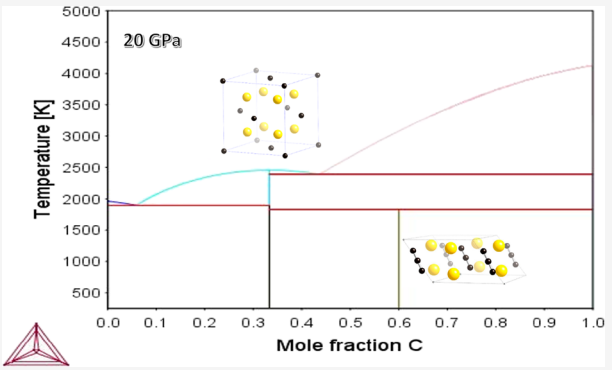

INTRODUCTION

The magnesium−carbon system at ambient pressure is believed to be simple[1] due to the absence of observable interactions between elements and metastability of known carbides.[2] The phase diagram suggests degenerated eutectic equilibrium between simple substances, hcp-Mg and graphite, and has a quite simple topology. Recent simulations of the phase diagram at ambient pressure with analysis of metastable equilibria have been reported in 2012 using the Calphad method,[3] and experimental values of solubility of C in liquid Mg[4] are in good agreement with modeling suggesting a value of zero for the binary interaction parameter for Mg−C liquid.

At the same time, two magnesium carbides, α-Mg_2C_3 and MgC_2, can be obtained (without high pressure, HP) only by nonequilibrium chemical routes[5] in the Mg−C−H or Mg−C−O−H[6] systems with participation of organic compounds (e.g., CH_4, C_2H_2, and C_5H_{10}). α-Mg_2C_3 has an orthorhombic crystal structure,[7] while MgC_2 crystallizes in tetragonal syngony.[8] Both carbides are metastable up to quite high temperatures, while their thermochemical study has shown that both compounds have no domains of thermodynamic stability at ambient pressure.[2] Later *ab initio* studies have shown that a high pressure does not make them thermodynamically stable.[9] So, the formal use of the reported experimental high-temperature (HT) (meta)stability domains of magnesium carbides at ambient pressure may lead to alternative phase diagrams[10] with a eutectic of high Mg content contradicting experimental observations.[4]

The first HP formation of Mg_2C_3 from MgC_2 was reported as early as 1983.[11] The evolution of the Mg−C phase diagram at high pressures has attracted attention because it is one of the systems for synthesis of diamond with particular electronic properties.[12,13] This system still remains very promising for the directed search of new superhard materials with advanced properties such as superconductivity, etc.[14] At the same time, the phase diagrams proposed,[15] although explaining correctly the domains of liquid−diamond equilibria at high temperatures, are unsatisfactory in the low- and medium-temperature ranges since they are based on the weakly supported hypotheses of MgC and MgC_2 compounds,[12] not confirmed by later crystallochemical studies of the Mg−C system at high pressures (Table 1).[9,16,17]

The full suite of magnesium carbides has been accomplished quite recently by a methodology of complementary *ab initio* simulations and experimental exploration of the metal−C system at high-pressure, high-temperature (HPHT) conditions (Table 1). Two magnesium carbides, monoclinic β-Mg_2C_3[9] and cubic antifluorite Mg_2C,[16] become stable at high pressures and can be recovered at ambient conditions. The composition and the crystal structure of these high-pressure compounds have been confirmed by a large variety of characterization techniques.

Received: October 12, 2022
Revised: December 19, 2022
Published: January 20, 2023

Table 1. Crystallographic Data for Phases of the Mg−C System at Ambient Conditions

phase and reference(s)	Pearson notation/ structure	lattice parameter(s) (Å)	remarks
hcp-Mg	hP2/hcp	a = 3.209	used for calculation of HPHT equilibria
		c = 5.2101	
dhcp-Mg	hP4/dhcp	a = 3.209	HP phase of Mg; neglected for equilibria calculations (thermodynamic properties similar to hcp-Mg)
		c = 10.420	
Mg_2C[16]	cF12/Na_2O	a = 5.4480	Used for calculation of HPHT equilibria
MgC[12a]	cF8/NaCl	a = 5.635	reported HP phase never confirmed, probably confused with NaCl (a = 5.635−5.641 Å) of the sample environment in the HP cell
α-Mg_2C_3[7]	oP10/Mg_2C_3	a = 3.209	metastable or unstable at the studied p−T range
		b = 3.209	
		c = 5.2101	
Mg_2C_3[2]		a = 7.43	ambient pressure phase(s) reported without the resolved crystal structure; most probably coincide with α-Mg_2C_3
		c = 10.59	
β-Mg_2C_3[9]	$mS10$/Mg_2C_3	a = 4.831, b = 4.700, c = 6.029, β = 126.71°	used for calculation of HPHT equilibria
γ-Mg_2C_3	see the text	see the text	used for calculation of HPHT equilibria
MgC_2[8]	tP6/MgC_2		metastable or unstable at the studied p−T range
MgC_2[2,5a]	tI6/CaC_2	a = 4.86	ambient pressure phases reported without the resolved crystal structure; most probably coincide with tP6-MgC_2
		c = 5.67	
	t[12a]	a = 5.54	
		c = 5.02	
C graphite	hP4/graphite	a = 2.4704	the 2H polytype was used for calculation of HPHT equilibria
		c = 6.7244	
C diamond	cF8/diamond	a = 3.5669	the 3C polytype was used for calculation of HPHT equilibria

[a]The existence of distinct phase(s) of this composition and crystal structure has not been confirmed.

In the present paper, we propose the refined set of thermodynamic parameters that allows obtaining the phase diagram of the Mg−C system up to 20 GPa and ∼4000 K using the Calphad method with a number of parameters refined based on our numerous experimental *in situ* and *ex situ* data. The calculated phase diagrams show satisfactory quantitative agreement with experimental p−T domains of thermodynamic stability for β-Mg_2C_3, γ-Mg_2C_3, and Mg_2C carbides. We correctly predict the p−T domain of diamond crystal growth (i.e., the equilibrium of diamond with Mg−C liquid). Qualitative agreement with previously suggested topologies at ambient and high pressures has been also established.

EXPERIMENTAL METHODS

As starting materials, Mg (Sigma Aldrich, 99.5%), glassy carbon (Sigma Aldrich, 99.95%), and graphite (Sigma Aldrich, 99.7%) were used. Samples were prepared under an argon atmosphere.

HPHT experiments up to 6 GPa and 2000 K were performed using the Paris-Edinburgh press (PE) at IMPMC (*ex situ*) and at SOLEIL (*in situ*). Opposite anvils of tungsten carbide and standard gaskets of pyrophylite or boron-epoxy (pressure medium) were used to compress the reaction volume to high pressures. A resistive furnace of graphite was used for heating at high pressures for 0.5−1 h in the *ex situ* and up to 10 h in the *in situ* experiments. The Mg−C mixtures were typically placed into an MgO capsule or (rarely) into a graphite heater. Pressure and temperature estimations were made either using calibrations obtained *ex situ* and *in situ* by Si and Mg melting,[18,19] thermocouple measurements, and using equations of states of Mg,[18] hBN,[20] MgO,[21] and Si.[22]

HPHT experiments up to 20 GPa and 2000 K were performed using multianvil presses at the EPL-CIW for *ex situ* studies and at ESRF for *in situ* observations.[23] Tungsten carbide truncated-cube anvils and standard MgO gaskets (pressure medium) were used. Graphite and reheaters were used to heat the compressed Mg+C mixtures in MgO capsules. The heating time was similar to PE experiments. Pressure and temperature estimations were made either using calibrations obtained *ex situ* and *in situ* by Si and Mg melting, phase transitions in silicates,[24] or by direct thermocouple measurements, and using equations of states of Mg,[18] MgO,[21] and Si.[22]

X-ray diffraction phase analysis was performed using a Rigaku Rapid diffractometer employing Mo Kα radiation and a curved area detector (at EPL-CIW), as well as using a diffractometer PANALYTICAL X'Pert Pro MTD with a Cu anode source. The absence of Mg+C interactions up to Mg melting (during at least) was confirmed by *in situ* observations at high temperatures under vacuum conditions (typically 1−5 Pa) that were performed using an HTK 1200N high-temperature oven chamber (Anton Paar) for conventional diffractometry (PANALYTICAL X'Pert Pro MTD).

In situ measurements in the PE cell were performed at the beamline PSICHÉ of the SOLEIL synchrotron. The phase transformations were primarily observed by energy-dispersive X-ray diffraction (2θ = 8°). After the crystallization of the new phase, a CAESAR system was used to collect the data and consisted of energy−angle diagrams permitting identification of new structures and removal of artifacts. Several energies ($\Delta E/E$ < 5%) were binned to obtain high-resolution angle-dispersive data. The system was calibrated using an Au standard.

In situ multianvil diffraction patterns were obtained at the beamline ID06 of ESRF. Angular-dispersive X-ray diffraction patterns were collected with a wavelength of λ = 0.3874 Å, and a scintillation counter served as the detector. The system was calibrated using a LaB_6 standard. Phase recognition of diffraction patterns was performed using PowderCell.[25]

https://doi.org/10.1021/acs.jpcc.2c07176
J. Phys. Chem. C XXXX, XXX, XXX−XXX

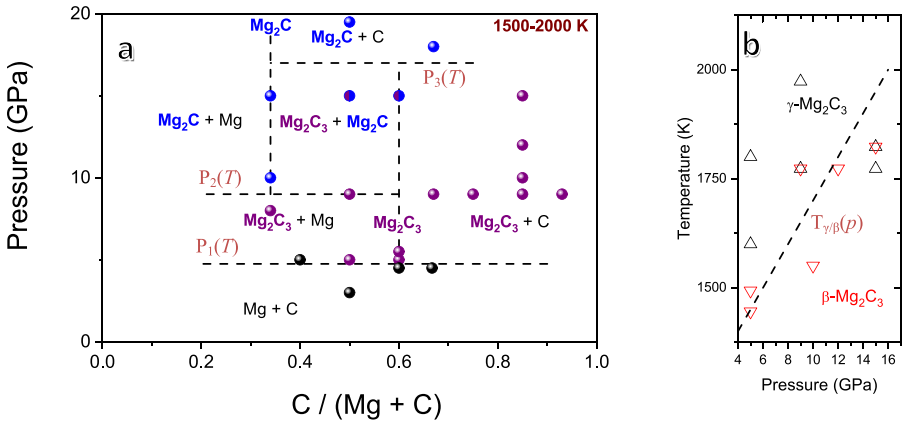

Figure 1. Experimental results on phase transformations and chemical reactions in the Mg−C system at HPHT conditions: (a) $p-x$ domains of magnesium carbide stabilities at 1500−2000 K (dashed lines are guide for the eyes) and (b) $p-T$ domains of stability of β- and γ-Mg_2C_3 (the dashed line shows the approximate boundary between the two polymorphs).

Thermodynamic Modeling Methods. The phase equilibria calculations were carried out using Thermo-Calc software.[26] Thermodynamic data of phases of the Mg−C system at ambient pressure were taken from ref 3.

At ambient pressure, no stable liquid carbon phase exists; however, at high pressures of interest, its contribution to the phase diagram is important. All gaseous phases were suspended in order not only to simplify the diagram, but also to easily compare it to the HP counterpart. The liquid Mg−C phase was described using the ideal solution model at ambient pressure, i.e., $\Delta H_{mix} = 0$ with entropy of mixing ΔS_{mix} equal to the ideal solution value; while $\Delta V_{mix} \neq 0$ allowed us to take into account nonideal behavior at high pressures. Solid phases were described in the framework of compound energy formalism (CEF).[27] Pressure dependencies of molar volumes were represented using the Murnaghan approximation.[28] Bulk moduli, their pressure derivatives, and thermal expansion coefficients for simple substances and compounds were taken from previous experimental measurements: Mg,[18] Mg_2C,[17] β-Mg_2C_3,[9] diamond, graphite, and liquid carbon.[29] The data for liquid Mg were found on the basis of the p,T melting curve of magnesium.[18,30] Previous *ab initio* results have shown that β-Mg_2C_3 has formation enthalpy (at 0 K) close to that of the α-Mg_2C_3 phase;[9] so, for the β phase, we used available thermodynamic data for the α phase at ambient pressure. The expression $G_{Cliquid} = G_{graphite} + 100{,}000 - 24.21 \cdot T$ was adopted from ref 31 instead of the expression $G_{Cliquid} = G_{graphite} + 117{,}369 - 24.63 \cdot T$ because of more reasonable agreement with the experimental melting p,T curve of graphite,[29] which results in the liquid−graphite−diamond triple-point parameters—11.2 GPa and 4140 K (instead of 12.4 GPa and 4700 K).

The molar volume of the liquid phase was described by the following equation:

$$V_L = V_{Mg}x_{Mg} + V_C x_C + \Delta V^{mix} x_{Mg} x_C$$

where $\Delta V^{mix} = -5 \times 10^{-6}$ m^3/mol is the mixing volume, which was found in the way to fix the changing of Mg_2C melting from incongruent to congruent at 15 GPa and 2250 K.

While at temperatures just above 1500 K, β-Mg_2C_3 forms from the mixture of elements at pressures above 5 GPa, higher temperatures show the formation of another phase, which we will denote here as γ-Mg_2C_3. The phase forms C_3H_4 after hydrolysis and has a ^{13}C NMR spectrum similar to the β-Mg_2C_3 phase. The powder XRD pattern of γ-Mg_2C_3 (Figure S2) shows some similarities to α-Mg_2C_3 and can be simulated (in order to easily recognize the phase in recovered samples) using a P-1 subgroup of β-Mg_2C_3 with a modified tilt of C_3^{4-} anions in relation to crystal planes. However, the exact crystal structure seems to be more complicated and has not been resolved so far. The experimentally established p,T curve of β-Mg_2C_3 to γ-Mg_2C_3 transformation (Figure 1b) allowed us to fix the free energy of γ-Mg_2C_3 as $G_{\gamma\text{-}Mg2C3} = G_{\beta\text{-}Mg2C3} + 20{,}000 - 20 \cdot T$ (J/mol).

There are no data on the energy of the Mg_2C formation in the literature. In the present study, the expression $G_{Mg2C} = 3/5 \times G_{\beta\text{-}Mg2C3} + 9000 - 8.0 \cdot T$ J/mol was assumed to fix the temperature interval of the existence of Mg_2C as 1100−1750 K at 10 GPa that was observed experimentally in our *in situ* experiments at ID06 at ESRF.

Parameters of the pressure dependencies of Gibbs energy of the phases in the Mg−C system are listed in Table 2.

RESULTS AND DISCUSSION

The pressure−concentration isothermal sections of the Mg−C phase diagram are presented in Figure 2. Two isotherms, 1500 and 1900 K, are illustrated that correspond respectively to (i) the experimentally observed onset of Mg+C interactions at ∼5 GPa (T_{int} of ∼1500−1550 K)[9] and (ii) the low boundary of diamond crystallization at ∼7.7 GPa (T_{diam} above 2000 K).[12] The principal domains of phase stability observed (Figure 1a) are satisfactorily reproduced. The onset pressure of Mg_2C_3 formation is ∼5 GPa (P_1 at Figure 1a, compare to Figure 2 and Figure S3), the pressure range in which diamond is in equilibrium with liquid is between 6 and 8 GPa, which agrees well with a previous report on diamond synthesis in this system.[15]

The evolution of the phase diagram (isobar sections) of the Mg−C system with pressure is shown in Figures 3−5. In addition to the quantitative changes of the diagram parameters (equilibria temperatures and limiting solubilities), variations of the diagram topology are observed, i.e., the incongruent type of Mg_2C melting transforms to the congruent one at about 15.5 GPa, and the L + C ⇄ Mg_2C_3 peritectic reaction changes to the Mg_2C + C ⇄ Mg_2C_3 peritectoid one above 16 GPa.

The comparison of theoretical and experimental results (for more details, see Figure S3 for superposition of experimental data of Figure 1a with isothermal sections of the phase diagram of Figure 2) shows the following:

https://doi.org/10.1021/acs.jpcc.2c07176
J. Phys. Chem. C XXXX, XXX, XXX−XXX

Table 2. Parameters of the Pressure Dependencies of Gibbs Energy[a]

phase	V_0, m^3/mol	B, GPa	B'	α, K^{-1}
graphite	5.259×10^{-6}	33.3	12.0	$2.32 \times 10^{-5} + 5.7 \times 10^{-9} \times T$
diamond	3.412×10^{-6}	588	5.0	$2.32 \times 10^{-6} + 1.0 \times 10^{-8} \times T$
C_{liquid}	7.626×10^{-6}	6.25	2.0	$2.32 \times 10^{-5} + 5.7 \times 10^{-9} \times T$
Mg_{hcp}	13.98×10^{-6}	37.0	4.2	9.5×10^{-5}
Mg_{liquid}	15.34×10^{-6}	40.0	4.2	5.5×10^{-5}
β-Mg_2C_3	33.03×10^{-6}	103.1	4.0	4.0×10^{-5}
γ-Mg_2C_3	34.5×10^{-6}	103.1	4.0	4.0×10^{-5}
Mg_2C	24.2×10^{-6}	87.0	5.1	6.0×10^{-5}

[a]Formally*, the parameters can be interpreted as V_0—the molar volume extrapolation to 0 K at 0.1 MPa; $B = -(\partial p/\partial \ln(V))_T$ and $B' = (\partial B/\partial p)_T$—bulk modulus and its first pressure derivative of the Murnaghan approximation; $\alpha = (\partial \ln(V)/\partial T)_p$—volume thermal expansion coefficient. *These parameters for elements were (principally) mutually adjusted to fit melting curves using equations and do not always coincide with more common values obtained by fitting the $V(p,T)$ data.

- β-Mg_2C_3 is unstable at atmospheric pressure and stabilizes at ~5 GPa. In our experiments, the β-Mg_2C_3 formation was observed only at 5 GPa and heating above 1500 K[9] i.e., at high enough temperature for the formation of the liquid phase in the system (Figure 4a).
- Mg_2C_3 forms from metastable MgC_2 and remains stable up to 1720 K at 6 GPa,[11] well in agreement with Figures 2 and 4a (i.e., present as a solid at 6 GPa at the isotherm diagram section of 1500 K and not at 2000 K).
- Diamond crystallization occurs at pressures above 7.7 GPa (well in agreement with previous reports[12,13,15]) where it stabilizes equilibrium of diamond with the liquid phase. It corresponds to incongruent melting of γ-Mg_2C_3 at 1990 K (Figure 2b).
- Thermodynamic stabilization and experimental formation of Mg_2C occur at pressures above 9 GPa (Figure 2a), well in agreement of previous *in situ* observations of Mg_2C decomposition.[17]
- The formation of Mg_2C_3 was not observed at pressures above 17 GPa. There was only Mg_2C present in the quenched samples. According to the calculated phase diagram, Mg_2C_3 does not have equilibrium with the liquid phase and completely disappears at high temperatures (~2000 K). The kinetics of interactions of Mg_2C with carbon is not sufficient to provide the formation of β-Mg_2C_3 at temperatures below 2000 K according to the $Mg_2C + C \rightleftarrows Mg_2C_3$ reaction.

The ambient pressure phase diagram has been calculated without considering the gaseous phases and from this point of view can be considered like a thermodynamic extrapolation from high pressures (since the parameters of interactions in the liquid phase and HP compounds have been adjusted using experimental data obtained at HP). $T_0(p)$ corresponds to the eutectics close to Mg melting, $L \rightleftarrows Mg + C_{gr}$ at ~0 at. % of Mg at ambient pressure. Previous experimental results also indicate that this eutectic is degenerated, in agreement with the low chemical affinity between graphite and magnesium and low mutual solubilities.

Below 5 GPa, no formation of magnesium carbide has been observed experimentally. Our calculations indicate the stability of Mg_2C_3 below 1000 K at 3 GPa, i.e., below Mg melting, which explains why formation of carbide has not been observed experimentally from elements at such a pressure.

$T_1(p)$ is the temperature of decomposition of high-pressure polymorphs of Mg_2C_3 (similar to decomposition of metastable α-Mg_2C_3 at ambient pressure). Above this temperature, carbon can be in direct contact with Mg-bearing liquid, and the single crystal growth of a stable carbon allotrope is possible. At 5 GPa, T_1 is close to diamond-to-graphite transformation, and thus, diamond growth does not occur.

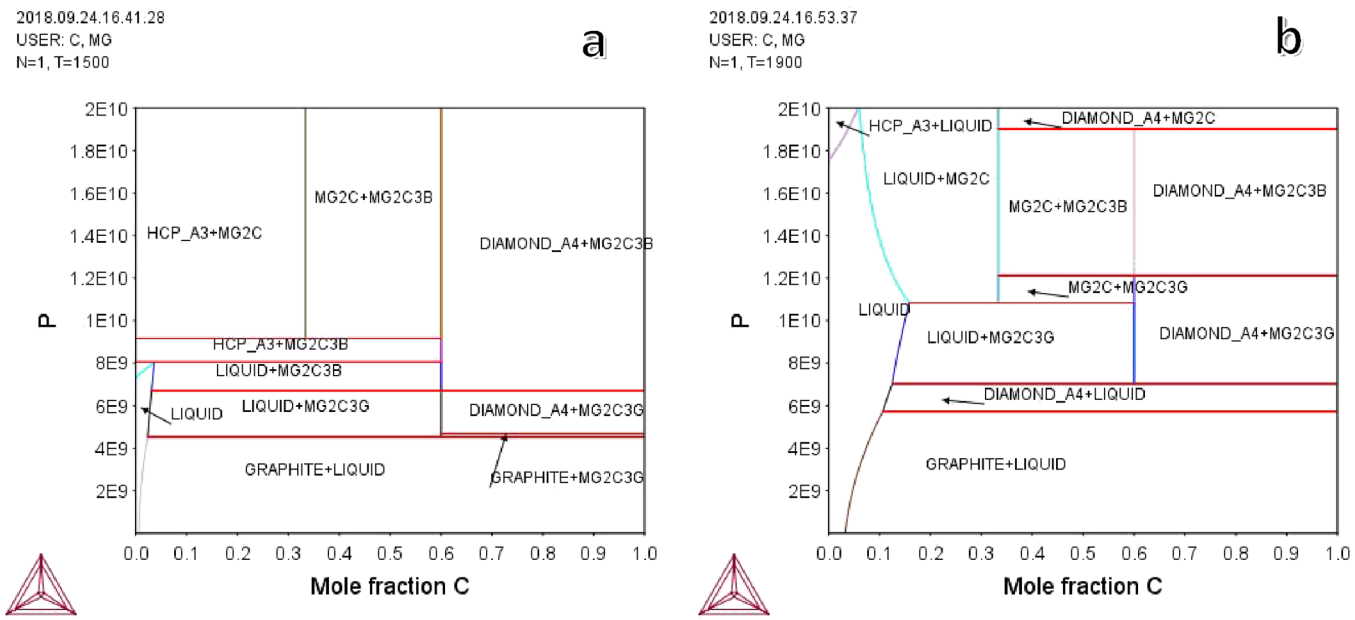

Figure 2. Calculated $p-x$ isotherm sections of the Mg−C phase diagram at 1500 (a) and 1900 K (b).

https://doi.org/10.1021/acs.jpcc.2c07176
J. Phys. Chem. C XXXX, XXX, XXX−XXX

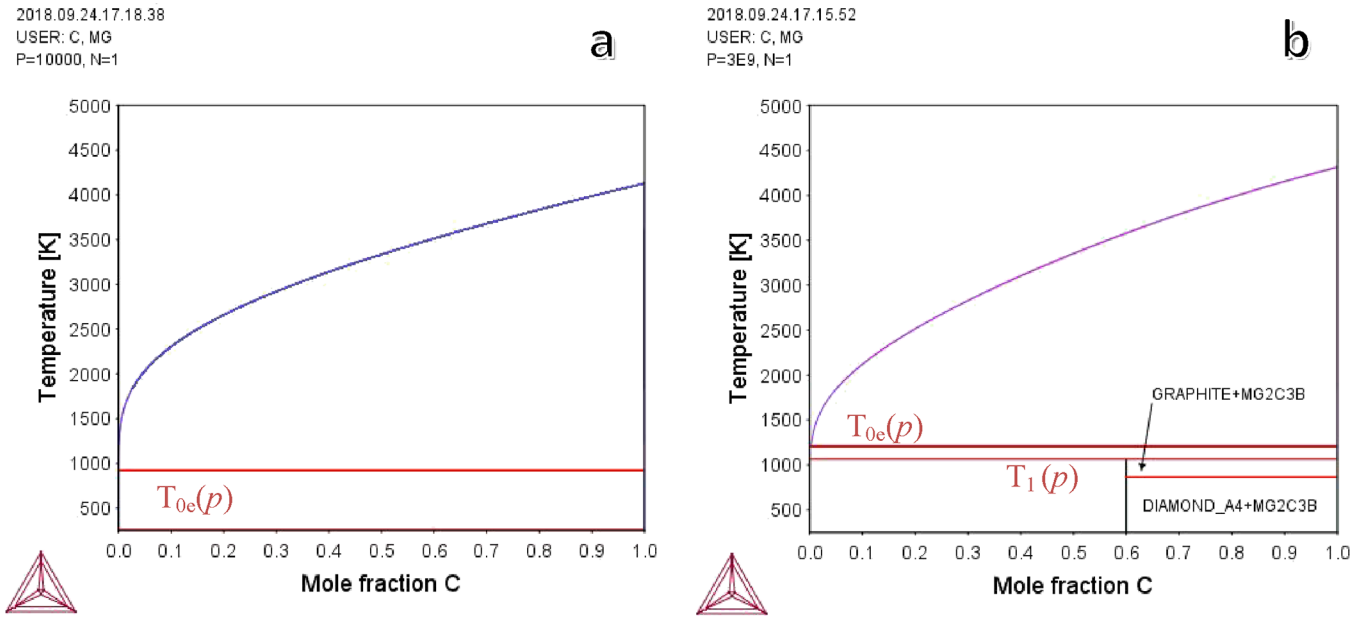

Figure 3. Phase diagram of the Mg−C system: isobar $T-x$ sections at 0.1 MPa (a) and 3 GPa (b). No magnesium carbide formation is expected below 1500 K at any pressure.

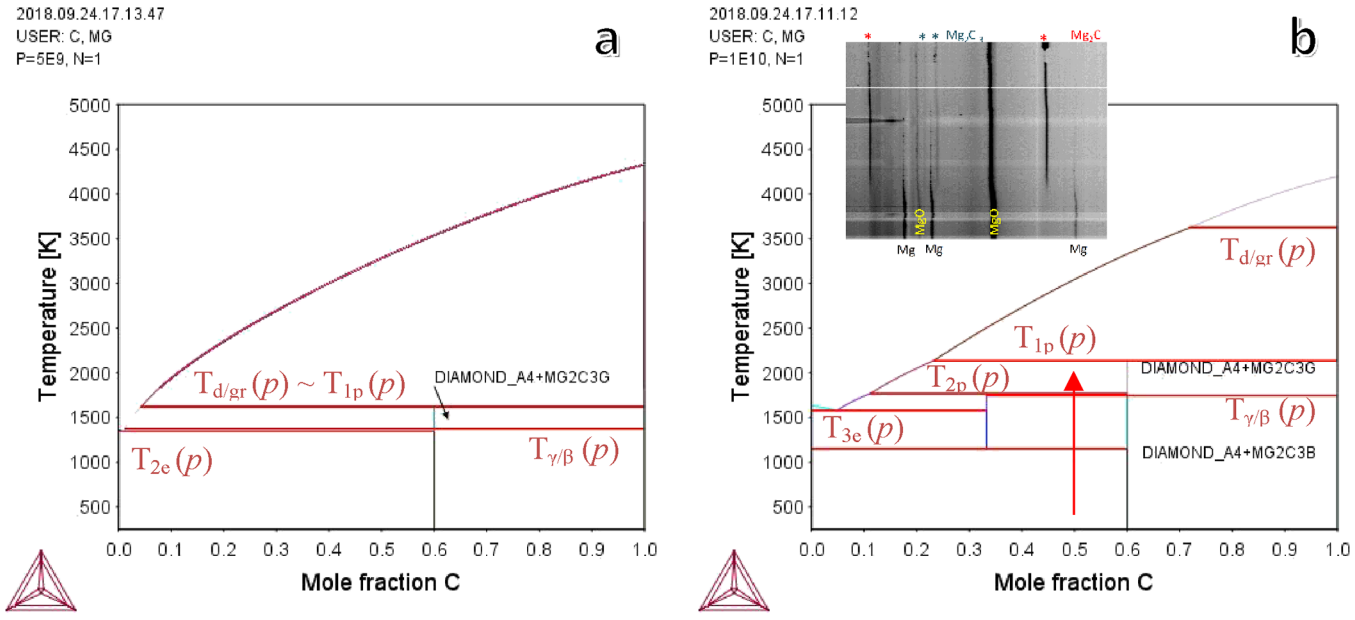

Figure 4. Phase diagram of the Mg−C system: isobar $T-x$ sections at 5 (a) and 10 GPa (b). The inset shows *in situ* XRD collected during heating at 9 GPa of the Mg+C mixture (ID06 beamline at ESRF). Formation and crystal growth of Mg_2C_3 and Mg_2C are possible, as well as liquid−diamond equilibrium.

The calculations predict the stability of β-Mg_2C_3 from at least 3 GPa at low temperatures; however, the low atomic diffusion rate prevents the interaction. The diamond stability range is also located at low temperatures rendering diamond growth impossible (diamond formation requires the presence of a liquid Mg−C phase).

At 5 GPa, the β-Mg_2C_3 stability attains the temperatures where the interaction occurs at a reasonable rate (~1500 K), which has been observed experimentally.[9] Diamond is only in thermodynamic equilibrium with carbide, and the temperature is not sufficient for the observable rate of solid-state diamond growth. The C−Mg eutectic remains degenerated. The calculated $T_1(p)$ of ~1600 K is in agreement with a quite high experimental value of the Mg_2C_3 decomposition temperature of ~1700 K at 6 GPa.[11]

$T_{2e}(p)$ indicates the temperature of the eutectic of Mg_2C_3 and Mg, and calculations show that it is already close to ~5% at 10 GPa. Eutectic behavior was experimentally observed at 8 GPa. The eutectic composition has been reported at 12 at. % C at 7.7 GPa and 1250 K and peritectic at 15%,[12] somewhat higher than our predicted values of 5 and 12 at. %.

Starting from 9 GPa, the experimental observation of Mg_2C becomes possible and has been observed *in situ* in a quite narrow temperature range, over the dominated β-Mg_2C_3 that forms at lower temperatures. β-Mg_2C_3 is predicted to stable up to ~1750 K (Figure 1b); above this temperature that the HT

https://doi.org/10.1021/acs.jpcc.2c07176
J. Phys. Chem. C XXXX, XXX, XXX−XXX

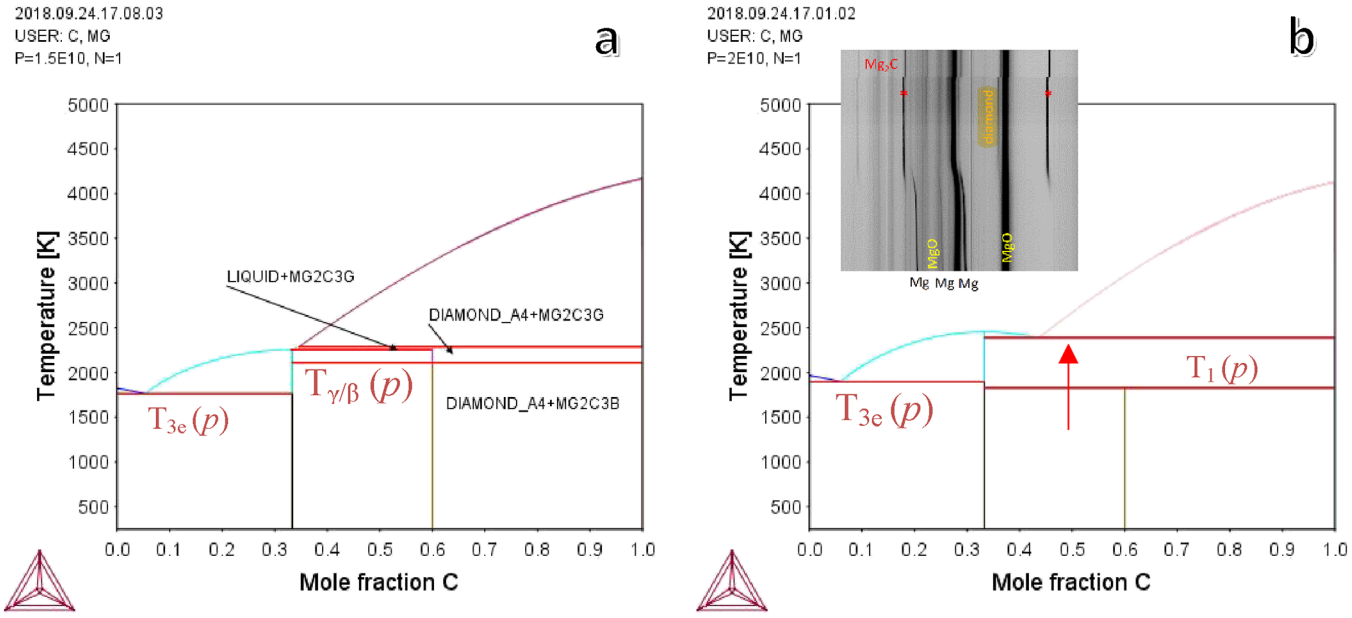

Figure 5. Phase diagram of the Mg−C system: isobar $T-x$ sections at 15 (a) and 20 GPa (b). The inset shows *in situ* XRD collected during heating at 19 GPa of the Mg+C mixture (ID06 beamline at ESRF). Mg_2C becomes the only stable carbide with congruent melting above 20 GPa and the HT domain.

forms, γ-Mg_2C_3 becomes stable. The diamond stability range increase in temperature and diamond synthesis in the Mg−C system becomes possible at ∼7.7 GPa.[12]

The calculated phase diagram at 10 GPa (Figure 4b) indicates the extended equilibrium domain between diamond and liquid phases, well in agreement with experimental observations of single crystal diamond growth at ∼7.7 GPa.[13] At 10 GPa, the topology of the phase diagram remains the same. High-temperature stability of the Mg_2C phase was observed, well in agreement with our experiments. At 15 GPa, we predict that Mg_2C melts congruently, and this result agrees with our experiments on the *ex situ* Mg_2C synthesis of the pure phase at ∼15 GPa.[16] Our previous observations of the Mg_2C phase during decompression at 1500 K down to ∼8−10 GPa[17] and its formation during heating at ∼9 GPa (inset of Figure 4b) agree well with the peritectic character of Mg_2C decomposition predicted by our simulations.

At 15 GPa (Figure 5a), the stability domain of graphite disappears completely, while the Mg_2C compound becomes stable from low temperatures to its congruent melting at ∼2250 K.

The calculated phase diagram at 20 GPa is shown at Figure 5b. Mg_2C is predicted to melt at ∼2500 K and is stable at all temperatures below melting. Mg_2C_3 is stable up to 1800 K, i.e., at temperatures below Mg melting, well in agreement with the fact that we observed only Mg_2C with diamond in our HPHT experiments on synthesis above 17 GPa.

In situ XRD probing of the Mg−C mixture (Mg:C = 1:1) under heating at 19(1) GPa has shown that diamond crystallizes together with Mg_2C at ∼1750(250) (inset of Figure 5b), i.e., without an intermediate of the liquid phase (according to the isobar section at 20 GPa, Figure 5b). This mechanism is possible only at a high enough pressure. Such a phase diagram, together with *in situ* observations, explains the easier synthesis of the Mg_2C phase above 15 GPa. Mg_2C_3 formation was not clearly observed in our experiment at 19(1) GPa, most probably because of the instability of both β and γ polymorphs above the Mg melting. Once quenched, which typically leads to the pressure drop (down to ∼10 GPa), reheating showed the formation of a noticeable amount of Mg_2C_3 (always together with Mg_2C), well in agreement with our phase diagram at 10 GPa (Figure 4b).

CONCLUSIONS

As a result of our *in situ* and *ex situ* studies of the Mg−C system, only two magnesium carbide compounds Mg_2C_3 (in β and γ forms) and Mg_2C participate in phase equilibria at HPHT conditions up to 20 GPa and melting temperatures. The existence of some previously suggested carbides has been disproven. Using this data, the Mg−C phase diagram has been revised by adjusting the observations to thermodynamic CALPHAD simulations. The domains of thermodynamic stabilities of Mg_2C_3 and Mg_2C show satisfactory agreement with numerous experiments of magnesium carbides' syntheses at HPHT conditions, while the $p-T$ range of possible growth of single crystal diamond agrees well with the calculated domain of diamond−liquid coexistence.

ASSOCIATED CONTENT

Supporting Information

The Supporting Information is available free of charge at https://pubs.acs.org/doi/10.1021/acs.jpcc.2c07176.

Phase diagrams of carbon and magnesium; Mg−C phase diagrams compared with experimental data; hypothetical crystal structure of γ-Mg_2C_3 and its powder XRD pattern (PDF)

AUTHOR INFORMATION

Corresponding Author

Alexandre Courac − *UMR CNRS 7590, Muséum National d'Histoire Naturelle, IRD UMR 206, Institut de Minéralogie, de Physique des Matériaux et de Cosmochimie (IMPMC), Sorbonne Université, 75005 Paris, France; Earth & Planets Laboratory, Carnegie Institution of Washington, Washington,*

https://doi.org/10.1021/acs.jpcc.2c07176
J. Phys. Chem. C XXXX, XXX, XXX−XXX

District of Columbia 20015, United States; Institut Universitaire de France (IUF), 75005 Paris, France; orcid.org/0000-0002-1249-5325;
Email: alexandre.courac@sorbonne-universite.fr

Authors

Vladimir Z. Turkevich − *UMR CNRS 7590, Muséum National d'Histoire Naturelle, IRD UMR 206, Institut de Minéralogie, de Physique des Matériaux et de Cosmochimie (IMPMC), Sorbonne Université, 75005 Paris, France; National Academy of Sciences of Ukraine, Institute for Superhard Materials (ISM), 04074 Kiev, Ukraine*

Carlos Renero-Lecuna − *UMR CNRS 7590, Muséum National d'Histoire Naturelle, IRD UMR 206, Institut de Minéralogie, de Physique des Matériaux et de Cosmochimie (IMPMC), Sorbonne Université, 75005 Paris, France; Bionanoplasmonics, CIC biomaGUNE, 20014 San Sebastian, Spain;* orcid.org/0000-0002-3160-1795

Yixuan Zhao − *UMR CNRS 7590, Muséum National d'Histoire Naturelle, IRD UMR 206, Institut de Minéralogie, de Physique des Matériaux et de Cosmochimie (IMPMC), Sorbonne Université, 75005 Paris, France*

Yann Le Godec − *UMR CNRS 7590, Muséum National d'Histoire Naturelle, IRD UMR 206, Institut de Minéralogie, de Physique des Matériaux et de Cosmochimie (IMPMC), Sorbonne Université, 75005 Paris, France;* orcid.org/0000-0002-9221-7076

Timothy A. Strobel − *Earth & Planets Laboratory, Carnegie Institution of Washington, Washington, District of Columbia 20015, United States;* orcid.org/0000-0003-0338-4380

Wilson A. Crichton − *ESRF-The European Synchrotron, 38000 Grenoble, France*

Nicolas Guignot − *Synchrotron SOLEIL, 91192 Gif-sur-Yvette, France*

Hicham Moutaabbid − *UMR CNRS 7590, Muséum National d'Histoire Naturelle, IRD UMR 206, Institut de Minéralogie, de Physique des Matériaux et de Cosmochimie (IMPMC), Sorbonne Université, 75005 Paris, France*

Ioannis Touloupas − *UMR CNRS 7590, Muséum National d'Histoire Naturelle, IRD UMR 206, Institut de Minéralogie, de Physique des Matériaux et de Cosmochimie (IMPMC), Sorbonne Université, 75005 Paris, France*

Complete contact information is available at: https://pubs.acs.org/10.1021/acs.jpcc.2c07176

Author Contributions

V.Z.T. and A.C. performed calculation of the phase diagram; A.C. and T.A.S. performed experiments at EPL; C.R.-L. and H.M. performed experiments at IMPMC; A.C., Y.L.G., W.A.C., Y.T., and T.A.S. performed experiments at ESRF; A.C., Y.L.G., and N.G. performed experiments at SOLEIL; this paper was written by the contribution of all authors.

Notes

The authors declare no competing financial interest.

■ ACKNOWLEDGMENTS

A.C. and Y.L.G. thank Agence Nationale de Recherche for financial support (project ANR-17-CE08-0038). C.R.-L. thanks the LabEx MATISSE program AAP 2016-POST-DOCTORANTS. The *in situ* XRD experiments were performed on the beamline ID06-LVP at the European Synchrotron Radiation Facility (proposals CH-5431 and CH-5787) and at the PSICHÉ beamline at the synchrotron SOLEIL (proposal 20130222). We are grateful to Drs. J. Guignard and K. Spektor at the ESRF for providing assistance in using the beamline ID06-LVP. V.Z.T. thanks Centre Nationale de Recherche Scientifique (CNRS) for financial support (DIALOG 2017).

■ REFERENCES

(1) SpMCBN, C-Mg. Data from SpMCBN refractory alloy databases. In *The Spencer Group SpMCBN Database for Carbide, Nitride, Boride and Silicide Systems* at http://www.crct.polymtl.ca/FACT/phase_diagram.php?file=C-Mg.jpg&dir=SpMCBN, 2018.
(2) Irmann, F. Zur Kenntnis der Magnesiumcarbide. *Helv. Chim. Acta* **1948**, *31*, 1584−1602.
(3) Chen, H.-L.; Schmid-Fetzer, R. The Mg−C phase equilibria and their thermodynamic basis. *Int. J. Mater. Res.* **2012**, *103*, 1294−1301.
(4) Chen, H.-L.; Li, N.; Klostermeier, A.; Schmid-Fetzer, R. Measurement of carbon solubility in magnesium alloys using GD-OES. *J. Anal. At. Spectrom.* **2011**, *26*, 2189−2196.
(5) Rueggeberg, W. H. C. The Carbides of Magnesium. *J. Amer. Chem. Soc.* **1943**, *65*, 602−607.
(6) Diaz, A. F.*Formation of magnesium metal and magnesium and calcium carbides by metal oxide reduction with methane*. Massachusetts Institute of Technology, 1997.
(7) Fjellvag, H.; Karen, P. Crystal structure of magnesium sesquicarbide. *Inorg. Chem.* **1992**, *31*, 3260.
(8) Karen, P.; Kjekshus, A.; Huang, Q.; Karen, V. L. The crystal structure of magnesium dicarbide. *J. Alloys Compd.* **1999**, *282*, 72−75.
(9) Strobel, T. A.; Kurakevych, O. O.; Kim, D. Y.; Le Godec, Y.; Crichton, W.; Guignard, J.; Guignot, N.; Cody, G. D.; Oganov, A. R. Synthesis of beta-Mg_2C_3: A Monoclinic High-Pressure Polymorph of Magnesium Sesquicarbide. *Inorg. Chem.* **2014**, *53*, 7020−7027.
(10) Hu, B.; Du, Y.; Xu, H.; Sun, W.; Zhang, W. W.; Zhao, D. Thermodynamic description of the C-Ge and C-Mg systems. *J. Min. Metall., Sect. B* **2010**, *46*, 97−103.
(11) Hájek, B.; Karen, P.; Brožek, V. Thermal decomposition of magnesium sesquicarbide. *Collect. Czech. Chem. Commun.* **1983**, *48*, 1963.
(12) Shul'zhenko, A. A.; Ignat'eva, I. Y.; Bel'avina, N. N.; Belousov, I. S. Constitution diagram of magnesium-carbon system at 7. 7 GPa. *J. Superhard Mater.* **1988**, *1988*, 3−5.
(13) Kovalenko, T. V.; Ivakhnenko, S. A. Properties of diamonds seed-grown in the magnesium-carbon system. *J. Superhard Mater.* **2013**, *35*, 131−136.
(14) Le Godec, Y.; Courac, A.; Solozhenko, V. L. High-pressure synthesis of superhard and ultrahard materials. *J. Appl. Phys.* **2019**, *126*, 151102.
(15) Novikov, N. V. New trends in high-pressure synthesis of diamond. *Diamond Relat. Mater.* **1999**, *8*, 1427−1432.
(16) Kurakevych, O. O.; Strobel, T. A.; Kim, D. Y.; Cody, G. D. Synthesis of Mg_2C: A Magnesium Methanide. *Angew. Chem., Int. Ed.* **2013**, *52*, 8930−8933.
(17) Kurakevych, O. O.; Le Godec, Y.; Strobel, T. A.; Kim, D. Y.; Crichton, W. A.; Guignard, J. High-Pressure and High-Temperature Stability of Antifluorite Mg_2C by in Situ X-ray Diffraction and ab Initio Calculations. *J. Phys. Chem. C* **2014**, *118*, 8128−8133.
(18) Courac, A.; Le Godec, Y.; Solozhenko, V. L.; Guignot, N.; Crichton, W. A. Thermoelastic equation of state and melting of Mg metal at high pressure and high temperature. *J. Appl. Phys.* **2020**, *127*, No. 055903.
(19) Jouini, Z.; Kurakevych, O. O.; Moutaabbid, H.; Le Godec, Y.; Mezouar, M.; Guignot, N. Phase boundary between Na-Si clathrates of structures I and II at high pressures and high temperatures. *J. Superhard Mater.* **2016**, *38*, 66−70.
(20) Kurakevych, O.; Solozhenko, V. High-Pressure Design of Advanced BN-Based Materials. *Molecules* **2016**, *21*, 1399.

(21) Dorogokupets, P. I.; Dewaele, A. Equations of state of MgO, Au, Pt, NaCl-B1, and NaCl-B2: Internally consistent high-temperature pressure scales. *High Press. Res.* **2007**, *27*, 431−446.
(22) Kurakevych, O. O.; Le Godec, Y.; Solozhenko, V. L. Integrated form of the Anderson-Gruneisen equation of state for p-V-T data fit: Application to the compounds of boron, carbon, silicon and some metals. *J. Phys.: Conf. Ser.* **2017**, *950*, No. 042023.
(23) Guignard, J.; Crichton, W. A. The large volume press facility at ID06 beamline of the European synchrotron radiation facility as a High Pressure-High Temperature deformation apparatus. *Rev. Sci. Instrum.* **2015**, *86*, No. 085112.
(24) Fei, Y.; Saxena, S. K.; Navrotsky, A. Internally consistent thermodynamic data and equilibrium phase relations for compounds in the system MgO-SiO_2 at high pressure and high temperature. *J. Geophys. Res.: Solid Earth* **1990**, *95*, 6915−6928.
(25) Nolze, G.; Kraus, W. PowderCell 2. 0 for Windows. *Powder Diffr.* **1998**, *13*, 256−259.
(26) Andersson, J.-O.; Helander, T.; Höglund, L.; Shi, P.; Sundman, B. Thermo-Calc & DICTRA, computational tools for materials science. *Calphad* **2002**, *26*, 273−312.
(27) Hillert, M. The compound energy formalism. *J. Alloys Compd.* **2001**, *320*, 161−176.
(28) Murnaghan, F. D. The compressibility of media under extreme pressures. *Proc. Nation. Acad. Sci. USA* **1944**, *30*, 244−247.
(29) Gustafson, P. An Evaluation Of The Thermodynamic Properties And The P-Phase T-Phase Diagram Of Carbon. *Carbon* **1986**, *24*, 169−176.
(30) Errandonea, D. The melting curve of ten metals up to 12 GPa and 1600 K. *J. Appl. Phys.* **2010**, *108*, No. 033517.
(31) Gurvich, L. V.; Weits, I. V.; Medvedev, V. A.; Khachkuruzov, G. A.; Yungman, V. S.; Bergman, G. A., *Thermodynamic properties of individual substances*. Press of AN SSSR: Moscow, 1979; Vol. *2*.

NOTE ADDED AFTER ASAP PUBLICATION

This paper was published ASAP on January 20, 2023, with author Carlos Renero-Lecuna's name spelled incorrectly. The corrected version was reposted on January 20, 2023.

https://doi.org/10.1021/acs.jpcc.2c07176
J. Phys. Chem. C XXXX, XXX, XXX−XXX